The stability and a.c. electrical characteristics of composites containing YBa$_2$Cu$_3$O$_{7-x}$ and alumina at elevated temperatures

A. OVENSTON, D. QIN, L. SHIELDS*, J. R. WALLS
*Department of Chemical Engineering, and *Department of Chemistry and Chemical Technology, University of Bradford, West Yorkshire, BD7 1DP, UK*

Samples of a high-temperature superconductor YBa$_2$Cu$_3$O$_{7-x}$ (orthorhombic phase) showed no significant weight loss in nitrogen up to 1173 K; however, differential thermal analysis measurements show that restructuring/decomposition begins around 1121 K. No reaction with alumina was found after prolonged heating at 1073 K. Electrical properties between 100 Hz and 1 MHz were generally stable at high temperatures, with little variation in properties at 1 MHz in inert and oxidizing atmospheres. Surface oxygen can be removed at high temperatures in flowing argon causing erratic electrical behaviour at lower frequencies and lower temperatures, which can be associated with changes in the oxygen content, x, and partial quenching to the high-temperature tetragonal phase. Stability and electrical tests after pretreatment of YBCO–alumina composites at 933 K in CO$_2$ or steam showed partial decomposition to BaCO$_3$, CuO and Y$_2$Cu$_2$O$_5$ and a phase transition from orthorhombic to tetragonal in the YBa$_2$Cu$_3$O$_{7-x}$. The original state could be retrieved by calcination in air at 1073 K.

1. Introduction

For most of the "high T_c" superconductors, oxygen is found to reversibly intercalate into the lattice which makes these materials potentially suitable as selective oxidation catalysts [1]. Klissurski and Rives [2] have recently published a comprehensive review of high-temperature superconductors in catalysis. They found no extraordinary catalytic properties could be associated with the unusual solid-state chemistry and physical properties of these materials, but that some of the related, but non-superconductive, cuprates showed extremely high efficiency in some important reactions, such as carbon monoxide oxidation. Further evaluation of the activity of such materials for the oxidative coupling of hydrocarbons is in progress. The possibility of using such conducting materials as catalysts for partial oxidation of methane reactions in a reactor heated by electromagnetic energy, has already been discussed [3, 4].

Owing to the ease of removal of partial lattice oxygen, YBa$_2$Cu$_3$O$_{7-x}$ (YBCO) is a feasible catalyst. However, its use may be limited by its susceptibility to chemical attack from the surrounding phases. The stability of YBCO not only depends on its oxygen content and structure, but also on the environment during and after calcination. YBCO shows metastable behaviour with respect to water, water vapour, carbon dioxide and some solvents [5]. Water and carbon dioxide are the two most likely species present in ambient air and in catalytic reactions. It is reported that YBCO reacts with water to form the non-

superconducting phase Y$_2$BaCuO$_5$, CuO and Ba(OH)$_2$ [6–8] with oxygen evolved simultaneously. Ba(OH)$_2$ will react with ambient CO$_2$ to form BaCO$_3$ [6, 7]. YBCO reacts with ambient CO$_2$ to form the Y$_2$Cu$_2$O$_5$ phase and other barium-rich compounds [9, 10].

There are distinct advantages of using electromagnetic energy to heat catalysts [3] which may be designed to absorb suitably energy from r.f. fields [4, 11]. In the case of YBCO, which is highly conducting at high temperatures, it is necessary to add an insulator such as alumina in order to attenuate the overall a.c. loss and so prevent the occurrence of thermal runaway. Between 50 and 70 wt % YBCO was considered to give the optimum composite and it is these compositions which have been investigated here. Consequently, it is important to ascertain whether or not any interaction between the YBCO and alumina will occur at elevated temperatures. Differential thermal analysis (DTA), thermogravimetric analysis (TGA) and X-ray diffraction (XRD) have been used to study the stability of YBCO alone and in the presence of α-Al$_2$O$_3$. The reactions of YBCO/Al$_2$O$_3$ composites with CO$_2$ and H$_2$O were studied at 933 K and are described below.

Lattice oxygen may also be lost from YBCO at high temperatures even in an inert atmosphere. Studies of a.c. behaviour in argon have been used to monitor this effect. A.c. electrical properties of YBCO/alumina composites in CO$_2$ atmospheres have also been studied and correlated with the stability tests.

2. Experimental procedure

Samples containing YBCO + α-Al$_2$O$_3$ were prepared as described previously [4]. Pellets containing 50 wt % YBCO with platinum enamel contacts fired on to the end faces of discs 1.2 cm diameter and about 3 mm thick were used for the a.c. electrical measurements. The effective net conductivity (reciprocal R) is about 25G where G is the conductance of the composite. Other a.c. parameters referred to are the dimensionless loss tangent, (tan $\delta = G/\omega C_p$, where C_p is the parallel capacitance), and the dielectric loss $\varepsilon'' \propto G/\omega$ [12]. Temperatures from ambient to 1073 K were investigated and frequencies between 100 Hz and 1 MHz were scanned. Gas flow rates were controlled using Brookes flow meters and a master controller. The experimental method has been described in detail elsewhere [12].

Computer-controlled Shimadzu DTA-50 and Shimadzu TGA-50 equipment were used for DTA and TGA investigations. Experiments were conducted with powdered samples containing 70 wt % YBCO in a platinum crucible with a nitrogen atmosphere passing at a flow rate of 30 ml/min^{-1}. A temperature range of 293–1173 K with a ramp of 30 K min^{-1} was employed. XRD measurements were carried out using a Siemens Diffractometer 500 with CuK$_\alpha$ radiation at room temperature. Stability tests were conducted on YBCO/Al$_2$O$_3$ composite powders (7:3 by weight) and on crushed pelleted samples A–E which had been subjected to the following pre-treatments:

A, calcination in air for 5 h at 1073 K;

B, calcination in CO$_2$ + Ar (10 and 50 ml min^{-1}, respectively) for 1 h at 933 K;

C, treatment B followed by calcination in air for 5 h at 1073 K;

D, 1 h at 933 K in argon bubbled at 10 ml min^{-1} through water, then cooled in dry argon;

E, treatment D followed by calcination in air for 5 h at 1073 K.

3. Results

3.1. Stability of YBCO alone and mixed with Al$_2$O$_3$

The DTA–TGA profiles of YBCO alone and with Al$_2$O$_3$ are shown in Fig. 1. According to TGA, neither sample showed significant weight changes from 293–1173 K. The DTA curve of YBCO shows two endothermic peaks below 373 K, one at 543 K, and a sharp endothermic curve from 1121 K. The YBCO is unaffected by the addition of Al$_2$O$_3$, because no significant difference was found between the two samples except that the peak at 543 K becomes obscure. YBCO with Al$_2$O$_3$ shows a somewhat steeper curve between 573 and 1073 K than YBCO alone; this is due to the change of heat capacity of the sample. The temperature of the sharp endothermic curve is reduced to 1108 K for YBCO with Al$_2$O$_3$ added. The XRD spectra of YBCO alone and with Al$_2$O$_3$ are shown in Fig. 2. The orthorhombic structure of YBCO appears clearly in both samples and is in agreement with the literature (e.g. [13]).

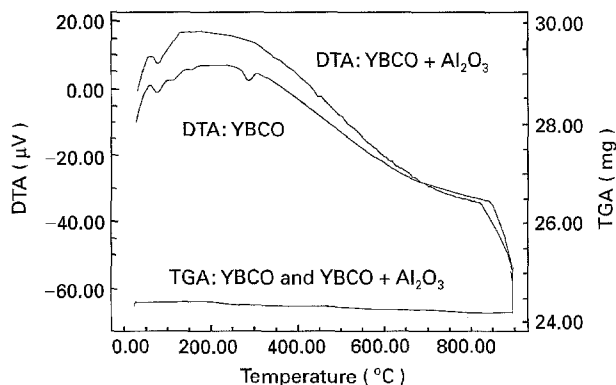In the XRD spectrum of sample A, there are two additional peaks which may be due to the presence of

Figure 1 DTA and TGA curves for YBCO and YBCO/alumina.

a Y$_2$Cu$_2$O$_5$ phase. The 100% peak for Y$_2$Cu$_2$O$_5$ is coincident with a YBCO phase peak and would not be observed. The principal observed peaks correspond to a 90% (2 0 4) reflection of Y$_2$Cu$_2$O$_5$ at 33.1° for the 2θ measurement. The other observed reflection is located at 28.8° which corresponds to the (0 0 4) reflection. No extra peak other than those associated with YBCO, Y$_2$Cu$_2$O$_5$ and Al$_2$O$_3$ are found in the spectrum for YBCO with Al$_2$O$_3$.

3.2. Electrical properties in air and argon

The conductance of a pellet containing 50 wt % YBCO in argon as a function of temperature is shown in Fig. 3a. At the lowest frequency of 100 Hz, behaviour is thermally activated over the entire temperature range with an activation energy of about 0.24 eV (1 eV ≃ 100 kJ mol^{-1}), which indicates that a hopping charge mechanism is dominant. For this amount of YBCO, neglecting voids, the volume fraction of the conducting component will be between about 41% and 49% depending on the density of the originally sintered YBCO. At this level it is likely to be close to the percolation threshold [14] and the subsequent effect of any dipole losses in the insulating component will have little effect, because mobile charges will be able to travel relatively easily throughout the structure. As the frequency is increased less temperature-dependent dipolar losses become apparent particularly at the lower temperatures. At the highest temperatures the conductance becomes virtually independent of frequency as the thermally activated charges dominate the loss processes.

With the passage of time, the conductance was found to decrease dramatically, particularly at the lower temperatures and lower frequencies as shown in Fig. 3b. Studies on further samples of this composite material showed similar behaviour. The inert argon stream is effectively carrying away oxygen, causing reduction of some of the surface layers at high temperatures and a consequent reduction in the mobile charge conductivity when the measurements are repeated. By re-oxidizing the samples in air at 973 K for 1 h, the original conductivity characteristics could be recovered.

The dielectric loss of the material in its original state at temperatures between ambient and 920 K is shown
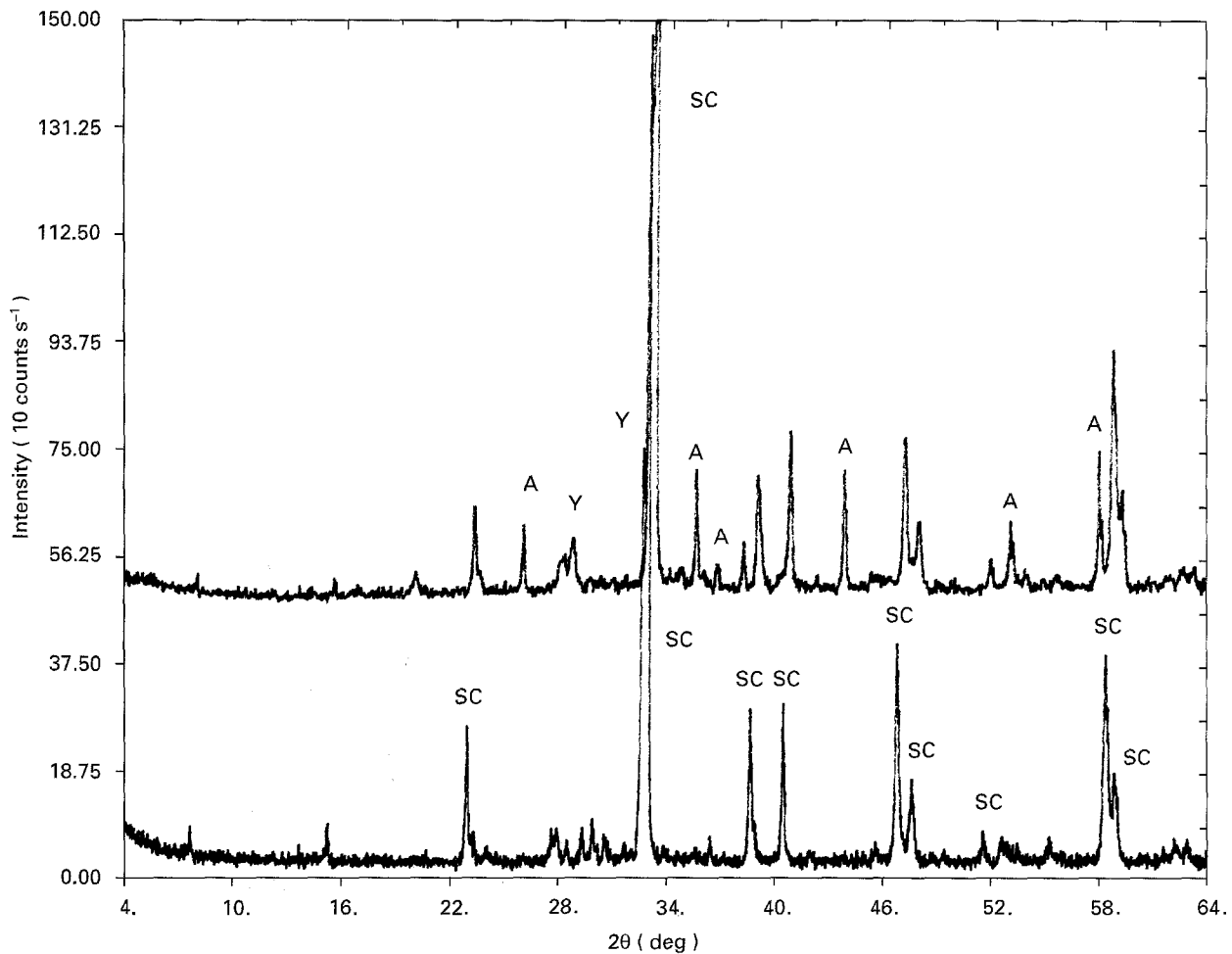
Figure 2 XRD spectra for YBCO and YBCO/alumina after calcination in air for 5 h at 1073 K. A, alumina; Y, $Y_2Cu_2O_5$; SC, superconductor YBCO(123).
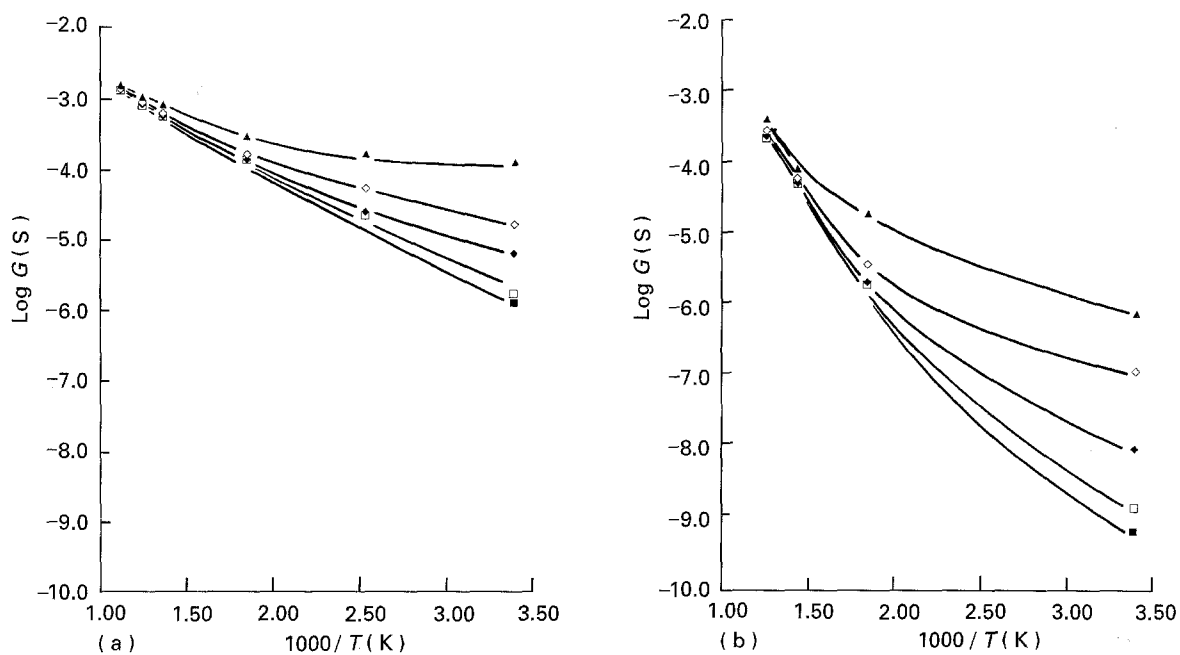

Figure 3 Conductance as a function of temperature and frequency for YBCO + 50 wt % alumina in argon. (a) Initial, (b) repeat. (■) 100 Hz, (□) 1 kHz, (♦) 10 kHz, (◇) 100 kHz, (▲) 1 MHz.

in Fig. 4. The parallel lines with a slope approaching — 1 are typical of materials of high dielectric loss in which thermally activated hopping charges are dominant. At 297 and 400 K the curves tend to flatten at the higher frequencies as other losses in the material

manifest themselves. There is also some indication of a superimposed dipolar-type loss process which is more clearly seen when log G is plotted as a function of log frequency (Fig. 5a). This loss peak occurs at higher frequencies as the temperature is increased,
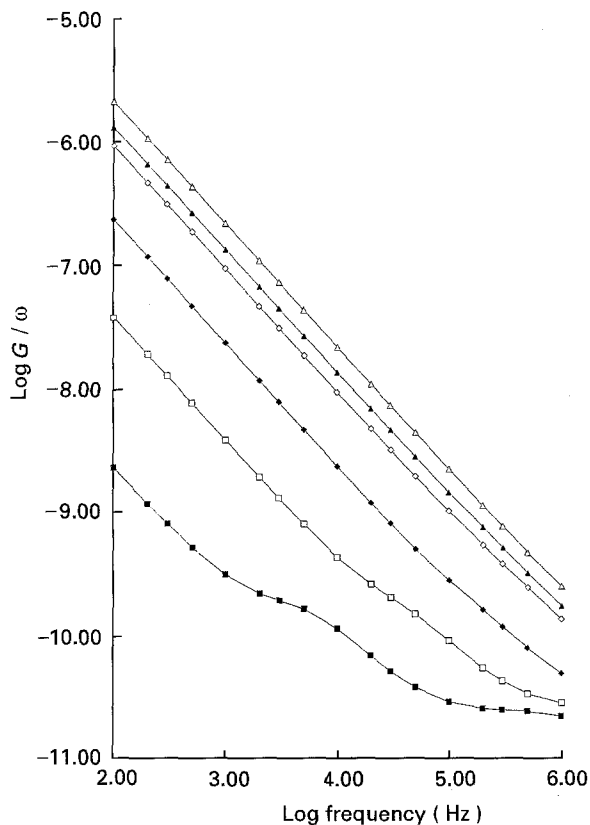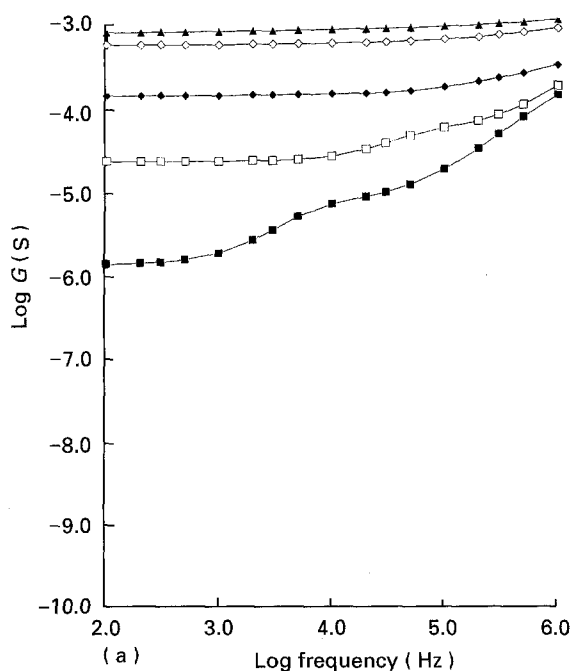
Figure 4 Initial dielectric loss for YBCO + 50 wt% alumina between 297 and 920 K. (■) 297 K, (□) 400 K, (◆) 550 K, (◇) 750 K, (▲) 825 K, (△) 920 K.

introduction of argon, almost immediate changes were observed. The geometry dependent loss tangent $(G/\omega C_p)$ clearly shows these changes to be greatest at the lower frequencies with major decreases occurring during the first 10 min (Fig. 6). However, at 1 MHz the changes are negligible over a period of 1 h. Thus for the purposes of maintaining a constant temperature in an r.f. field, changes in the atmosphere between air or an inert gas are likely to have a negligible effect.

3.3. The reaction of YBCO with CO_2

At low temperatures, CO_2 has little effect, for example at 455 K a gas mixture of CO_2 diluted in argon (flowing at 10 and 50 ml min^{-1}, respectively) had a negligible effect on the electrical properties, however, at 941 K, a rapid fall in the conductance occurred, as shown in Fig. 7. The conductance at all frequencies fell by an order of magnitude in 30 min and did not recover but remained at a steady level once the CO_2 had been turned off. The effect of this gas is thus not a reversible chemisorption process but one involving a chemical change. Further experiments on the stability of the material confirmed the nature of this change.

After exposure to CO_2 at 933 K for 1 h, sample B showed some new peaks in its XRD spectrum (Fig. 8b). Analysis of these peaks showed that they are due to CuO, $BaCO_3$, $Y_2Cu_2O_5$, Y_2CuBaO_5 and the tetragonal phase of YBCO [13, 15]. The appearance of these compounds shows that the YBCO has reacted with CO_2 under the given conditions. The products of the reaction indicated that the reaction is the partial decomposition of YBCO followed by further reaction with CO_2 and a phase transition from orthorhombic to tetragonal. The existence of the tetragonal phase of YBCO indicates that the reaction is not fast and probably proceeds slowly from the surface of the sample [9, 16–18]. No aluminium-containing
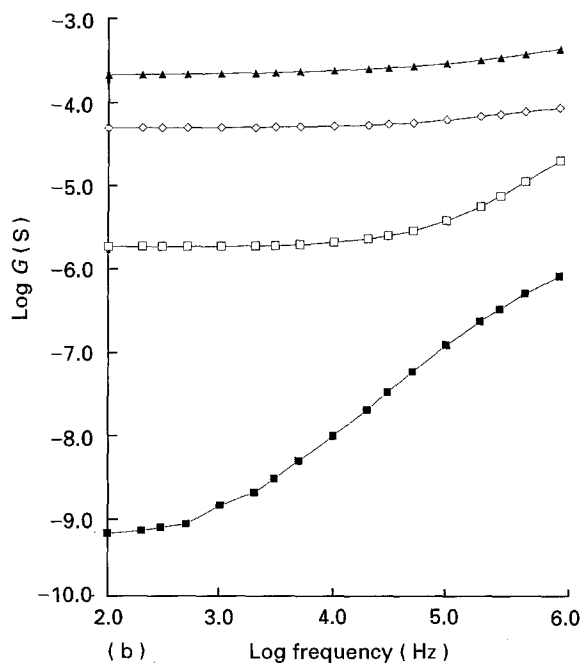
showing that this is also a thermally activated loss process. After repeating the experiment, the effect of frequency is more pronounced and the loss peak becomes displaced, Fig. 5b.

The electrical properties were monitored for a new sample as a function of time at 913 K. In air, the values of G and C_p remained stable for an hour, but with the

Figure 5 Conductance as a function of frequency and temperature for YBCO + 50 wt % alumina in argon. (a) Initial, (■) 297 K, (□) 400 K, (◆) 550 K, (◇) 750 K, (▲) 825 K; (b) repeat, (■) 297 K, (□) 555 K, (◇) 719 K, (▲) 827 K.
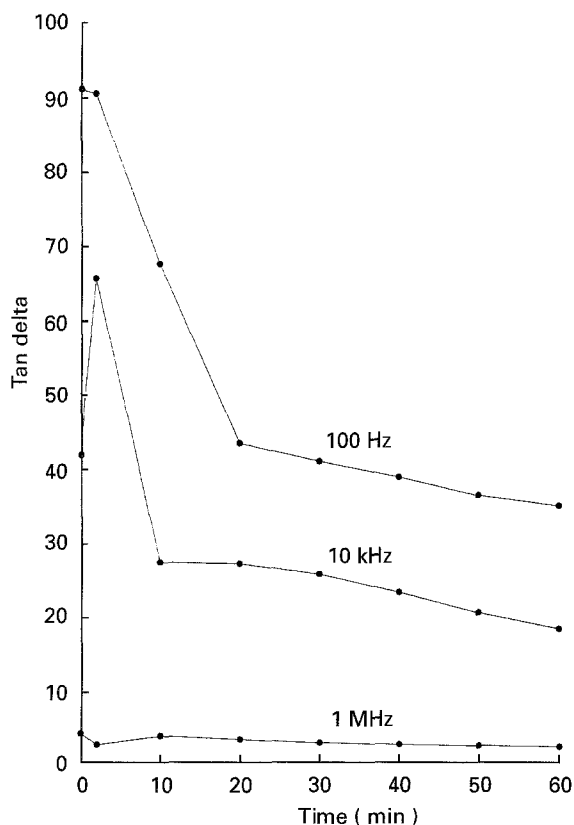
Figure 6 Loss tangent versus time for YBCO + 50 wt % alumina in argon at 913 K.

Figure 7 Conductance versus time for YBCO + 50 wt % alumina in CO_2 at 941 K.

compounds were found, which indicated that the Al_2O_3 constituent was not involved in the reaction.

After the material had been re-treated in air at 1073 K for 5 h (sample C), XRD showed most of the CuO and $BaCO_3$ had disappeared, but a small amount of $Y_2Cu_2O_5$ remained (Fig. 8c). When compared with sample A (Fig. 8a), both samples A and C showed similar spectra except for a slight difference in the peak height of $Y_2Cu_2O_5$. Thus it seems that the re-oxidation treatment is sufficient essentially to retrieve the structure of orthorhombic YBCO from the decomposition products and the phase transition.

3.4. Reaction of YBCO with water vapour at 933 K

After exposure to steam at 933 K for 1 h, sample D showed some new peaks in its XRD spectrum (Fig. 9d). Analysis of these peaks showed that they are due to CuO, $Ba(OH)_2$, Y_2BaCuO_5 or $Y_2Cu_2O_5$ and the tetragonal phase of YBCO [18]. The appearance of these compounds shows that the YBCO has reacted with steam under the given conditions. Again, the products of the reaction indicated that the reaction is the decomposition of YBCO and a phase transition from orthorhombic to tetragonal. As in the case of CO_2, no aluminium-containing compounds were found.

After the material had been re-treated in air at 1073 K for 5 h (sample E), the XRD spectrum showed most of the CuO and $Ba(OH)_2$ had disappeared but a small amount of $Y_2Cu_2O_5$ remained (Fig. 9e). When compared with sample A (Fig. 9a), both samples A
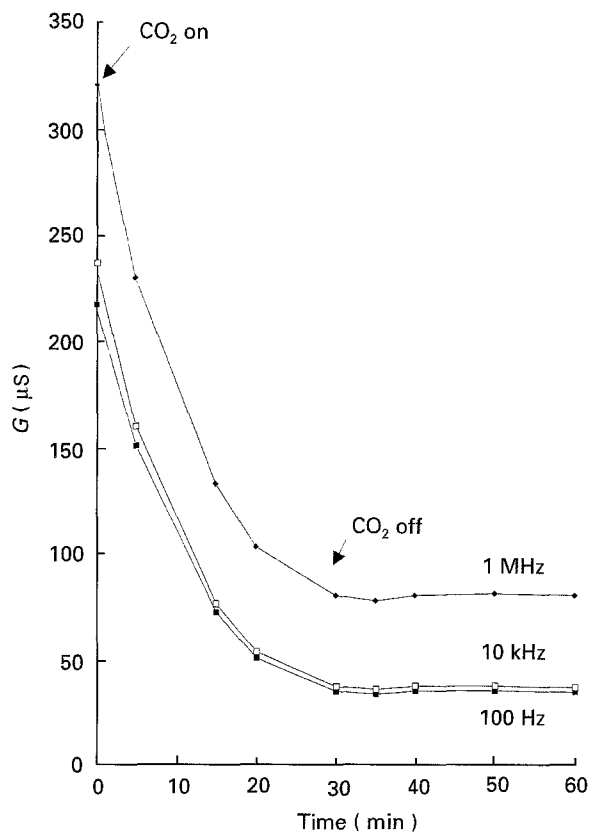
and C showed similar spectra except for a slight difference in the peak height of $Y_2Cu_2O_5$. Thus, after exposure to water vapour for 1 h the reoxidation treatment was sufficient for the original structure of the orthorhombic YBCO to be recovered.

4. Discussion

4.1. Stability of YBCO alone and with Al_2O_3

In the DTA of YBCO, the endothermic peaks before 573 K are due to the different sorts of adsorbed water on the surface or in the bulk. However, the endothermic curve from 1121 K is indicative of some reaction. Several authors have observed an endothermic peak at 1203–1223 K which is prior to the appearance of Y_2BaCuO_5 phase [9, 16–19]. It was suggested that the reaction corresponds to the decomposition of YBCO

$$YBa_2Cu_3O_{6+\delta} \rightarrow Y_2Cu_2O_5 + BaCuO_2 \quad (1)$$
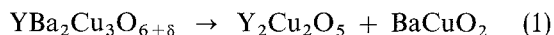
$BaCuO_2$ is not stable and will decompose to $BaCO_3$ and CuO at lower temperatures. The decomposition temperature observed here was lower than those temperatures reported elsewhere. Between 1073 K and the temperature of Reaction 1, there is no thermal reaction reported, the endothermic curve of YBCO at 1121 K (Fig. 1) probably corresponds to Reaction 1. The reason for the lower decomposition temperature is not clear. It is likely to be an effect of impurities, but their identification requires further study. Siva Prasad *et al.* [20] found that DTA/TGA and other properties strongly depended on the method of preparation of the material and concluded that a sol–gel method was superior to the rest.
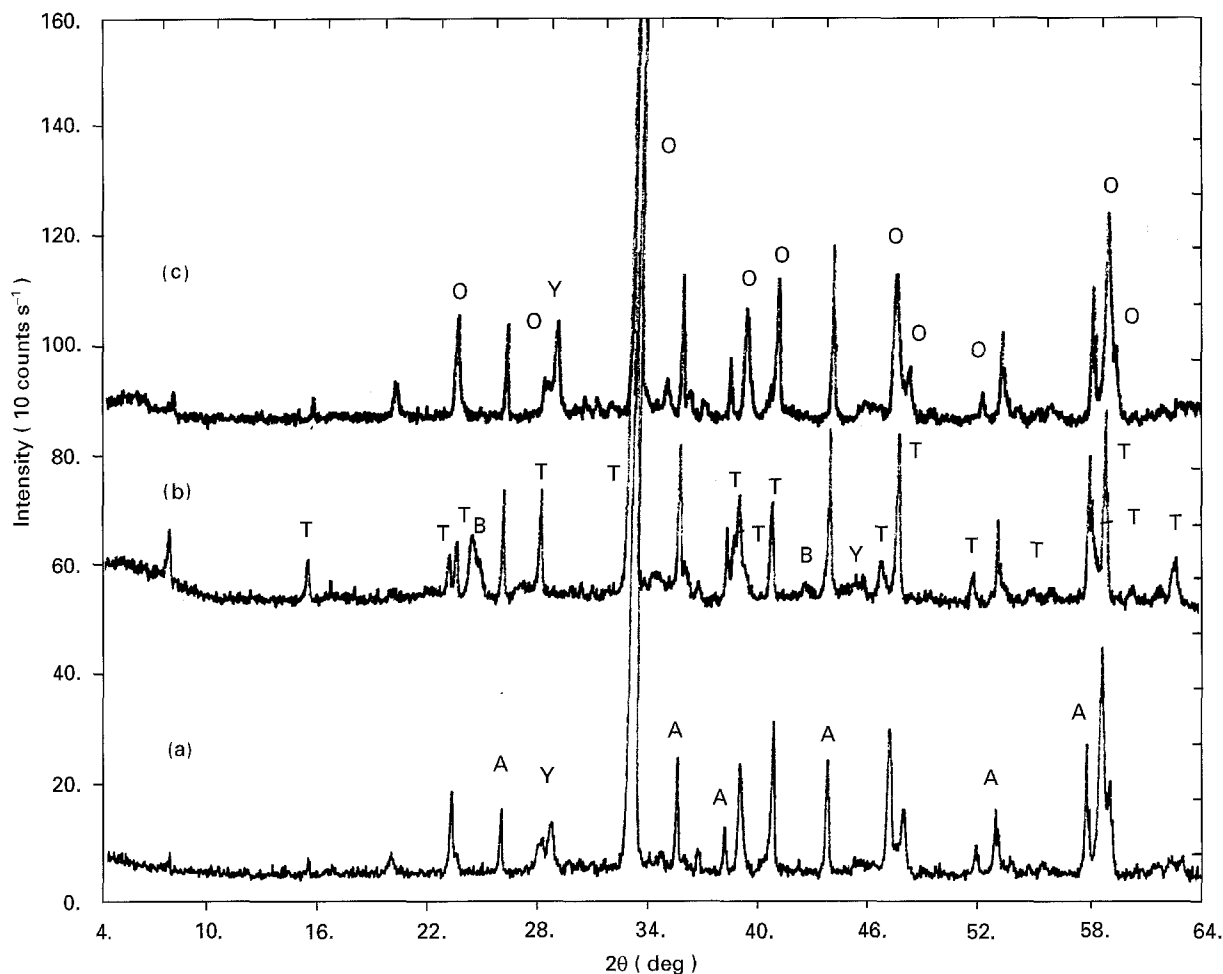
Figure 8 XRD spectra for YBCO/alumina after pretreatments a, b and c. (a) Calcination in air for 5 h at 1073 K, (b) calcination in CO_2 + Ar (10 and 50 ml min^{-1}, respectively) for 1 h at 933 K, (c) treatment B followed by calcination in air for 5 h at 1073 K. A, alumina; O, orthorhombic YBCO (123); T, tetragonal YBCO (123); B, $BaCO_3$; Y, $Y_2Cu_2O_5$ or Y_2CuBaO_5.

4.2. Electrical properties in air and argon
4.2.1. Phase changes

It is well known that YBCO undergoes a reversible tetragonal to orthorhombic structural phase transformation on changing the temperature or the oxygen content [15]. Above about 973 K it is in the tetragonal (T) phase, whereas below about 773 K it is in the orthogonal (O) phase [21]. The temperature for the O–T transition depends on the oxygen partial pressure. It is likely that the high-temperature T-phase may be quenched if the sample is rapidly cooled. Klissurski and Rives [2] consider the strength of the oxygen bond; a decrease in the oxygen content leads to an increase in the binding energy of oxygen evolved, the activation energy for oxygen desorption for the tetragonal phase being almost double that for the orthorhombic one. They suggest, therefore, that the T structure should exhibit a higher selectivity in partial oxidation, and that due to the essentially basic nature of the Y–Ba–Cu–O superconductors they should exhibit predominantly dehydrogenating activity. Bansal's TGA studies showed that a slow gain in weight occurred above about 538 K in oxygen and above about 700 K oxygen loss occurred even in oxygen [21]. Weight changes during heating and cooling are attributed solely to changes in the oxygen stoichiometry. On heating in nitrogen, weight was lost

continuously and slowly up to about 733 K, at a faster rate up to 1093 K, and much faster still above this temperature. It is therefore likely that a similar loss of oxygen will occur when YBCO is heated in an inert argon atmosphere as used in the experiments reported here and that if the sample is cooled quickly to room temperature, the high-temperature tetragonal state will be quenched and the YBCO will behave as a semiconductor. Furthermore, if, after conductivity measurements to high temperatures are made, the sample is not cooled slowly in air, the uptake of oxygen will not be complete and the original oxygen content not regained.

Nowotny *et al.* [22] derived a $T-P_{O_2}$ phase diagram covering temperatures between 300 and 1173 K and pressures between 10^2 and 10^5 Pa. Changes in activation energies but no discontinuities between the quasi-metallic O structure and the semiconducting T structure were observed and a p–n type transition was found within the semiconducting regime. At about 950–970 K in air, the compound should be in the T phase. Electrochemical oxygen titration was used to show that above about 800 K lattice oxygen continuously interacts with oxygen in the gas phase, but at lower temperatures, the oxygen content cannot be changed further in the bulk phase, but oxygen may still interact with thin surface and grain-boundary
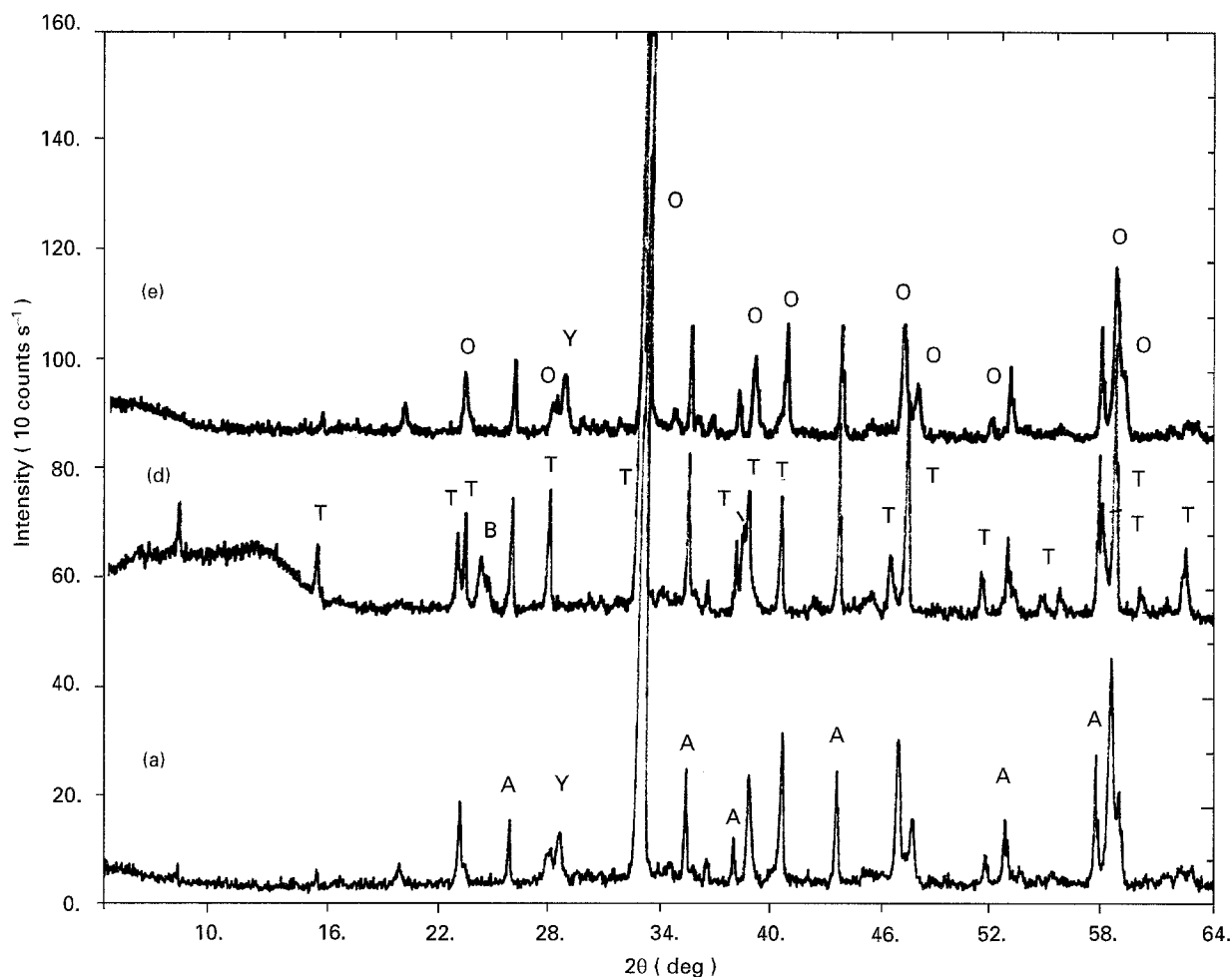
Figure 9 XRD spectra for YBCO/alumina after pretreatments a, d and e. (a) A, Calcination in air for 5 h at 1073 K; (d) D, 1 h at 933 K in argon bubbled at 10 ml min^{-1} through water, then cooled in dry argon; (e) treatment D followed by calcination in air for 5 h at 1073 K. A, alumina; O, orthorhombic YBCO(123); T, tetragonal YBCO(123); B, BaCO$_3$; Y, Y$_2$Cu$_2$O$_5$ or Y$_2$CuBaO$_5$.

layers. A comprehensive review of the electrical properties at elevated temperatures is given. Huang *et al.* [23] using e.m.f. measurements of a galvanic cell to measure the temperature dependence of Gibbs energy changes showed that the O–T phase transition may occur at 1025 K when the oxygen partial pressure is 1 atm. This temperature is somewhat higher than indicated in the phase diagram constructed by Nowotny *et al.* [22].

Changes in heat capacity between room temperature and 860 K have also helped clarify the phase transitions including changes from simple orthorhombic (OI) to orthorhombic (OII) structures, which for $x = 0.35$ occurs above about 700 K [24]. OII is an ordered orthorhombic phase in which full and empty Cu–O–Cu–O–. . . chains alternate giving rise to a supercell doubled along the a-axis. Yan *et al.* [25] reported resistive relaxation curves at constant temperature and constant composition, together with oxygen ordering studies by electron diffraction which suggest that in the range of composition $0.36 > x > 0$ at room temperature only the two orthorhombic varieties (whose perfect structures correspond to ideal composition $x = 0$ and $x = 0.35$, respectively), exist as thermodynamically stable phases. Relationships between temperature (673–1073 K) and composition, i.e. x, were determined for constant oxygen partial

pressures in N$_2$–O$_2$ mixtures with oxygen contents between 0.1% and 100%.

From these studies it is apparent that above about 673 K some lattice oxygen will be lost whatever the oxygen content of the atmosphere, and once x exceeds about 0.4 an O–T transition will occur as temperature is increased. This is the case in the treatment of YBCO/Al$_2$O$_3$ using CO$_2$ or H$_2$O with argon at 933 K. Owing to the lack of oxygen in the gas-flow, loss of lattice oxygen occurs and this eventually leads to an orthorhombic-to-tetragonal transition. After the calcination of sample B or D in air at 1073 K for 5 h, the orthorhombic structure is retrieved from the decomposed products and tetragonal structure. These results indicate that the uptake of oxygen from air under the given conditions is sufficient to re-establish the orthorhombic structure. The loss and gain of oxygen is reversible and dependent on the experimental conditions.

The O–T transformation will be accompanied by a change in the activation energy for electrical conductivity as the material changes slowly from a quasi-metallic state to a semiconducting state. The higher the P_{O_2} the higher will be the temperature of the transition. In air it is likely to occur at about 950 K but in a very low P_{O_2} it is closer to about 730 K. Thus, as the material is heated relatively quickly from a fully

oxidized state in argon, a conductivity with low activation energy is observed up to 920 K (Fig. 3a), because although the material loses some oxygen its O state may be retained. On maintaining the high temperature, oxygen will be lost, and on cooling rapidly in argon, the material will revert to tetragonal state at all temperatures if x is sufficiently high. Hence this explains the much reduced conduction and increased activation energies when the experiment is repeated in an argon atmosphere (Fig. 3b). The lost oxygen will not be retrieved unless the material is cooled extremely slowly in a high oxygen atmosphere, or reheated to about 673 K in air until maximum oxygen uptake is achieved. If higher temperatures are used to reoxidize the material the oxygen uptake will be more rapid due to the increased rate of diffusion of oxygen into the material but the amount of uptake will be reduced.

4.2.2. High-temperature conductivity

YBCO is a mixed conductor showing fast transport of oxygen ions, in addition to electronic conductivity at temperatures above 573 K. The ionic conductivity for oxygen ions has been measured for polycrystalline samples with porosities between 20% and 39% between 573 and 773 K [26]. This increases from about 10^{-3} to 10^2 S m^{-1} in air. The changes in activation energy observed around 663 K (2.2 $\pm$ 0.1 eV at low temperatures and 2.6 $\pm$ 0.1 eV at high temperatures) are probably associated with the decrease in oxygen content above this temperature. The temperature-dependent concentration of mobile oxygen defects basically determines the observed high-temperature activation energy. The electronic conductivity of YBCO increases with increasing P_{O_2} as more oxygen anion vacancies are formed; the concentration of all types of defect must be such that electrical neutrality is maintained. The sintering temperature was found to be extremely important for controlling the values of the defect concentrations in the oxygen sublattice and also in the metal sublattice.

Others have studied defect models and conduction mechanisms in more detail (e.g. [27, 28]). The electrical properties at elevated temperatures strongly depend on the extent of non-stoichiometry, x, and the resulting concentration of defects. Nowotny and Rekas [27] demonstrated that the hopping model can be used for the p-type semiconducting region, and for the n-type region (low P_{O_2}), the band model can be used. Su et al. confirm a p-type regime with a hopping conduction mechanism at high temperatures of 923–1123 K [28].

Within the stability region of the orthorhombic phase, the dominating defects are doubly ionized oxygen vacancies and electron holes [29]. With increasing deviation from stoichiometry the concentration of singly ionized oxygen vacancies increases and these dominate in the T phase. At high temperatures these should dissociate, producing free electrons whose concentration increases with increasing x. The mobility of the holes and its dependence on temperature in the orthorhombic phase was found to be reduced when

the value of x exceeded 0.4 in the tetragonal phase. A band model scheme was proposed. At $x \sim 0.7$ the appearance of an energy gap of order 1 eV takes place and for higher values of x transport takes place in more than one band and typical semiconductive properties can be observed.

Elschner et al. [30] have recently studied the time-dependent electrical resistance in order to determine the degree of oxidation. They emphasize that care must be taken in interpreting such experiments because atmosphere is interrelated with x. Thus large concentration gradients may be set up and affect the results. Their experiments were performed in well-defined P_{O_2} atmospheres. Activated processes such as barriers at grain surfaces did not affect the oxygen uptake which was detected down to 573 K, about 100 K lower than reported elsewhere.

Tuller and Opila [31] reviewed oxygen diffusion measurements up to 1990 and considered various defect models. Elschner et al. [30] later also considered the complex diffusion for which diffusion coefficients at 873 K between 10^{-3} and 10^{-8} m^2 s^{-1} have been quoted. These large variations may arise from many factors, such as anisotropy, diffusion along voids and cracks, grain boundaries or twin boundaries, porosity, grain size, initial oxygen stoichiometry, all of which may be partly dependent on the method of preparation, particularly the sintering temperature. MacManus et al. [32] performed measurements of oxygen-ion conductivity using an a.c. electrochemical impedance technique taking great care to correctly interpret their data from the resulting complex impedance diagrams. They determined the activation energy for oxygen-ion transport within the bulk of YBCO in air between 823 and 1043 K to be 1.5 $\pm$ 0.05 eV with typical conductivities of 5×10^{-3} and 6×10^{-1} S m^{-1} at these temperatures, respectively. At 1000 K the conductivity is about an order of magnitude lower than that of yttria-stabilized zirconia. Between 873 and 1098 K the activation energies for in-diffusion and out-diffusion at the surface were about 1.4 eV and 1.76 eV, respectively.

It is generally considerably more difficult to replace oxygen in YBCO than it is to remove it; the more dense the sample the greater being the difficulty [33]. The existence of some porosity has been found necessary for achieving both good oxidation (and fully orthorhombic state at room temperature) and low micro-cracking. Because a large surface area and the presence of small pores is imperative in a good catalyst, the presence of some porosity is likely to assist the diffusion of oxygen both in and out of the catalyst and simultaneously maintain a good catalytic activity.
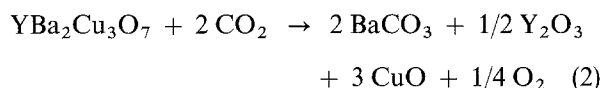
4.3. The reaction of YBCO with CO$_2$ and H$_2$O at 933 K

The high-temperature superconductor YBCO is reputed to react easily with both water vapour and carbon dioxide leading to decomposition of the lattice into $BaCO_3$, Y_2BaCuO_5 and CuO. At temperatures close to 573 K, the YBCO framework remains relatively unaffected, although a gradual decrease in the
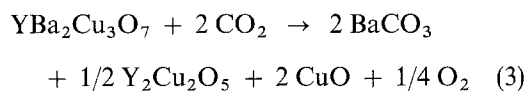
intensity of the main peaks indicating an "amorphization" of the catalyst has been reported [2]. XPS analysis of Y–Ba–Cu–O phases has shown that their surfaces are contaminated with degradation products such as $BaCO_3$, $Y(OH)_3$, Y_2BaCuO_5 and CuO due to reaction with atmospheric water and carbon dioxide. They note however, that the chemical reactivity towards water of $YBa_2Cu_3O_{6.6}$ is lower than that of $YBa_2Cu_3O_6$ and $YBa_2Cu_3O_7$. Pickering and Thomas [1], however, found that activity of YBCO for CO oxidation was maintained after 18 h and no new phases (e.g. carbonate formation and surface segregation) were detected, suggesting that any decomposition, if it occurs, is limited to the surface layer.

The decomposition of YBCO with CO_2 proceeds with measurable rates above 673 K. The products of the reaction are dependent on the reaction temperature [9, 10]. The decomposition reactions are considered to be

$$YBa_2Cu_3O_7 + 2\,CO_2 \;\rightarrow\; 2\,BaCO_3 + 1/2\,Y_2O_3$$
$$+ 3\,CuO + 1/4\,O_2 \quad (2)$$

and

$$YBa_2Cu_3O_7 + 2\,CO_2 \;\rightarrow\; 2\,BaCO_3$$
$$+ 1/2\,Y_2Cu_2O_5 + 2\,CuO + 1/4\,O_2 \quad (3)$$

Reaction 2 occurs below 1003 K and Reaction 3 above 1003 K. In fact, reaction 2 is the addition of Reaction 3 and the decomposition of $Y_2Cu_2O_5$

$$Y_2Cu_2O_5 \;\rightarrow\; Y_2O_3 + 2\,CuO \quad (4)$$
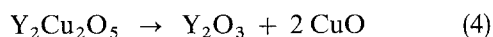
Because the change of $Y_2Cu_2O_5$ peak height and lack of Y_2O_3 were observed after the treatment of the sample, it seems likely that Reaction 3 occurs even at 933 K under the experimental conditions. The difference may be due to the use of argon rather than oxygen to dilute the CO_2. After the re-treatment of the sample in air for 5 h at 1073 K, the YBCO orthorhombic structure was retrieved. This implies that Reaction 2 or 3 is reversible under the conditions of the tests. Because CO_2 exists in air, some $Y_2Cu_2O_5$ remains in the sample.

The decomposition of YBCO with steam also proceeds with measurable rates above 673 K. The decomposition reactions are considered to be [13]

$$2\,YBa_2Cu_3O_7 + 3\,H_2O \;\rightarrow\; 3\,Ba(OH)_2$$
$$+ Y_2BaCuO_5 + 5\,CuO + 1/2\,O_2 \quad (5)$$
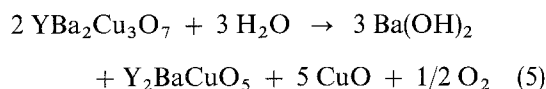
After calcination of the sample in air for 5 h at 1073 K, the YBCO orthorhombic structure was retrieved. This implies that Reaction 5 is reversible under the conditions of the tests. Again, due to the presence of some CO_2 in air, some $Y_2Cu_2O_5$ remains in the sample.

Because the tetragonal YBCO and the decomposition products co-exist after CO_2 and H_2O treatment (Figs 8 and 9) these processes involve the loss of oxygen from the orthorhombic YBCO, the phase transition from orthorhombic to tetragonal YBCO and the ultimate decomposition of both orthorhombic and tetragonal YBCO.

Tartaj et al. [33] found that a slow degradation of YBCO takes place at the material surface in contact with water vapour from air at room temperature after several days exposure. XPS experiments showed that $Ba(OH)_2$ apparently forms, giving rise to corresponding amounts of Y_2O_3 and CuO free oxides which subsequently react with water vapour to give YO(OH) and some $CuCO_3$. They found that subsequent oxidation was not able to regenerate the original stoichiometry in the surface region.

Temperature-programmed reduction experiments have shown that YBCO is less easily reduced than the non-conducting cuprates such as Ba_2CuO_5, $BaCuO_2$ and Y_2BaCuO_5 [2]. CO is relatively strongly held on YBCO; it only desorbs at 773 K with formation of CO_2. In a reducing atmosphere containing hydrogen at high temperatures, the CuO component is slowly reduced to copper.

Lin et al. [34] have recently studied the interaction of YBCO with CO, NO and H_2 + CO. CO resulted in the release of CO_2 at 400–800 K and the formation of $BaCO_3$ and reduction of Cu(II) and Y(III) above 800 K. With H_2 + CO, CO_2 and H_2O were produced below 830 K. At about this temperature, Cu(II) is reduced to Cu(I) and $BaCO_3$, the MeO group and the hydroxyl group were identified. At 1170 K, carbides could also be found on the YBCO surface. An active centre and mechanisms for these interactions were postulated to explain the high catalytic activity of YBCO. With such complex behaviour, detailed experiments involving simple oxidation reactions are required before the efficacy and long-term stability of YBCO in a reaction atmosphere can be assessed.

5. Conclusion

$YBa_2Cu_3O_{7-x}$ mixed with Al_2O_3 was analysed using DTA–TGA and XRD methods. No interaction was found between the YBCO and Al_2O_3 at either low or high temperatures. YBCO starts to decompose under a nitrogen flow at 1121 K. After calcination in air at 1073 K, $Y_2Cu_2O_5$ was found in the XRD spectrum.

In an inert atmosphere, surface oxygen is easily lost at high temperatures; this results in a reduction in conductivity at lower frequencies, but above about 950 K at 1 MHz, little change occurs, because here the a.c. behaviour is largely governed by dielectric losses associated with lattice dipoles. Thus for the potential use of such material for absorbing energy in an r.f. electromagnetic reactor, the high-temperature stability of the a.c. properties is an asset. Instability in the electrical properties at lower temperatures and, in particular, lower frequencies, is associated with the previous high-temperature history of the composite. The electrical properties largely depend on the degree of non-stoichiometry, x, which itself depends on the oxygen partial pressure and temperature. High x and low x are associated with the lower temperature semi-metallic orthogonal phase and the high-temperature semi-conducting tetragonal phase, respectively. Rapid cooling from high temperatures can result in some quenching of the tetragonal state and the observed

reduced conductivity, which can only be restored by reoxidation.

In a CO_2-rich atmosphere, the conductance falls irreversibly at high temperatures due to chemical changes. Treatment of YBCO with $CO_2:Ar = 1:5$ or steam at 933 K showed that an orthorhombic to tetragonal transition and a slow decomposition of YBCO occurs, the products of the decomposition being $BaCO_3$, CuO and $Y_2Cu_2O_5$ but without Y_2O_3. Following calcination of the sample in air at 1073 K, the YBCO structure was recovered.

The potential of such YBCO/alumina composites for catalytic oxidation reactions in an r.f. reactor has already been examined [3, 4]. Further work is underway to test the long-term stability and catalytic behaviour of the material both in a conventionally heated reactor and in reactors powered by electromagnetic energy.

References
1. I. J. PICKERING and J. M. THOMAS, *J. Chem. Soc. Farad. Trans.* **87** (1991) 3067.
2. D. KLISSURSKI and V. RIVES, *Appl. Cat. A: Gen.* **109** (1994) 1.
3. A. OVENSTON, J. R. WALLS, A. ALLEN and W. ARMSTRONG, *J. Mater. Sci.* **29** (1994) 1358.
4. A. OVENSTON, J. R. WALLS and D. SPRÎNCEANÃ, *J. Mater. Sci. Lett.* **14** (1995) 311.
5. G. DELL'AGLI, O. MARINO, G. MASCOLO, P. PERNICE, A. DI CHIARA, G. PEPE and U. SCOTTO DI UCCIO, *J. Mater. Sci: Mater. Electron.* **1** (1990) 20 (and references [1–7] therein).
6. I. M. LOW, S. S. LOW and C. KLAUBER, *J. Mater. Sci. Lett.* **12** (1993) 1574.
7. M. F. YAN, R. L. BARNS, H. M. O'BRYAN, Jr, P. K. GALLAGHER, R. C. SHERWOOD and S. JIN, *Appl. Phys. Lett.* **51** (1987) 532.
8. D. ZHUANG, M. XIAO and Z. ZHANG, *Solid State Commun.* **69** (1989) 179.
9. M. A. RODRIGUEZ, R. L. SNYDER, B. J. CHEN, D. P. MATHEIS, S. T. MISTURE, V. D. FRESHETTE, G. ZORN, H. E. GÖBEL and B. SEEBACHER, *Phys. C* **206** (1993) 43.
10. H. FJELLVÅG, P. KAREN, A. KJEKSHUS, P. KOFSTAD and T. NORBY, *Acta Chem. Scand.* **A42** (1988) 178.
11. A. OVENSTON and J. R. WALLS, *Trans. I. Ch. E.* **68** (1990) 530.
12. *Idem, J. Catal.* **140** (1993) 464.
13. J-P. ZHOU and J. T. McDEVITT, *Solid State Commun.* **86** (1993) 11.
14. A. OVENSTON and J. R. WALLS, *J. Phys. D Appl. Phys.* **18** (1985) 1859.
15. M. L. POST and G. PLEIZIER, *J. Solid State Chem.* **107** (1993) 166.
16. M. W. SHIN, T. M. HARE, A. I. KINGON and C. C. KOCH, *J. Mater. Res.* **6** (1991) 2026.
17. S. R. SU, M. O'CONNOR and M. LEVINSON, *ibid.* **6** (1991) 244.
18. A. I. KINGON, C. D. DAVIS, T. M. HARE, H. PALMOUR III, C. C. KOCH and D. G. HAASE, in "Proceedings of the Materials Research Society Symposium", **169** (Materials Research Society, 1990).
19. T. ASELAGE and K. KEEFER, *J. Mater. Res.* **3** (1988) 1279.
20. P. V. L. N. SIVA PRASAD, M. A. JALEEL, K. BHUPAL REDDY and V. N. MULAY, *J. Mater. Sci. Lett.* **9** (1990) 956.
21. N. P. BANSAL, *J. Mater. Res.* **3** (1988) 1304.
22. J. NOWOTNY, M. REKAS and W. WEPPNER, *J. Am. Ceram. Soc.* **73** (1990) 1040.
23. X. HUANG, L. CHEN, Y. HUANG and T. HUI, *Solid State Ionics* **40–41** (1990) 807.
24. T. MATSUI, T. FUJITA, K. NAITO and T. TAKESHITA, *J. Solid State Chem.* **88** (1990) 579.
25. Y. YAN, M-G. BLANCHIN, C. PICARD and P. GERDANIAN, *J. Mater. Chem.* **3** (1993) 603.
26. W. CARRILLO-CABRERA, H. D. WIEMHÖFER and W. GÖPEL, *Solid State Ionics* **32–33** (1989) 1172.
27. J. NOWOTNY and M. REKAS, *J. Am. Ceram. Soc.* **73** (1990) 1054.
28. M-Y. SU, C-E. ELSBERND and T. O. MASON, *ibid.* **73** (1990) 415.
29. J. MOLENDA, A. STOKLOSA and T. BAK, *Phys. C* **175** (1991) 555.
30. G. ELSCHNER, W. BECKER, H. D. WIEMHÖFER and W. GÖPEL, *Solid State Ionics* **32–33** (1992) 401.
31. H. L. TULLER and E. OPILA, *ibid.* **40–41** (1990) 790.
32. J. MacMANUS, D. FRAY and J. EVETTS, *Phys. C* **190** (1992) 511.
33. J. TARTAJ, C. MOURE, P. DURAN, J. L. GARCIA-FIERRO and J. COLINO, *J. Mater. Sci.* **26** (1991) 6135.
34. J. LIN, T. S. WEE, A. C. H. HUAN, K. L. TAN and K. G. NEOH, *J. Vac. Sci. Technol. A* **12** (1994) 2074.